

Measurement of the all-particle cosmic ray energy spectrum with IceTop

F. Kislak¹ for the IceCube collaboration²

¹DESY, Platanenallee 6, 15738 Zeuthen, Germany

²<http://www.icecube.wisc.edu>

Received: 2 November 2010 – Accepted: 19 January 2011 – Published: 19 May 2011

Abstract. IceTop is an air shower array at the geographic South Pole forming the surface component of the IceCube Neutrino Observatory. In this paper, a method to reconstruct shower size and primary energy spectrum from data measured by IceTop is described. Data were divided into three zenith angle bins. Using Monte Carlo based on the SIBYLL and Fluka hadronic interaction models, agreement with an isotropic flux can only be achieved under the assumption of a mixed composition. A preliminary all-particle energy spectrum is presented.

1 Introduction

The IceTop air shower array is currently under construction at the geographic South Pole as the surface component of the IceCube Neutrino Observatory (e.g. Achterberg et al., 2006). After completion in January 2011, it consists of 81 detector stations arranged on a triangular grid with a nominal spacing of 125m covering a total area of 1km². An IceTop station consists of two frozen water tanks with two Digital Optical Modules (DOMs) each to detect Cherenkov light produced by charged particles. IceTop is designed to detect air showers with primary energies between 500 TeV and 1EeV. Due to the high altitude of the South Pole plateau the atmospheric overburden is only about 700gcm⁻². Therefore, air showers in the energy range accessible by IceTop are close to their shower maximum when they reach the ground (e.g. Gaisser, 1990). This has several advantages: local shower density fluctuations are relatively small, and the dominant component of the air shower are photons and electrons.

The main goal of IceTop is the measurement of the energy spectrum and the chemical composition of cosmic rays around the “knee” (a change in the spectral index at ~ 3 PeV)

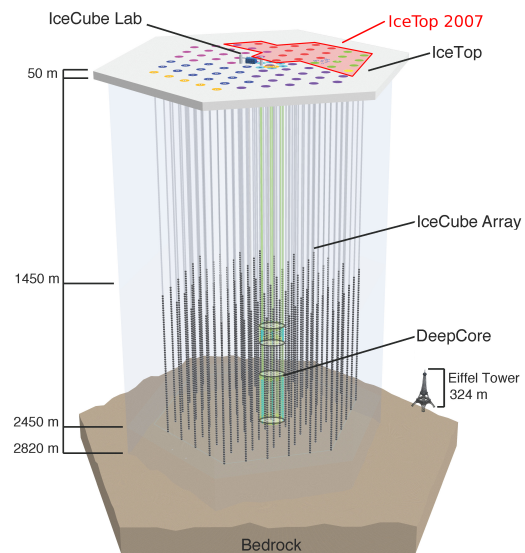


Fig. 1. The 79 string IceCube Observatory in January 2010. The 26 station IceTop array used in this analysis is outlined in red.

and above. In combination with IceCube, which can only be reached by muons with an energy of more than about 300GeV, IceTop provides a new handle on the primary mass by measuring the air shower parameters at the surface in coincidence with TeV muons reaching the deep detector.

In this paper, an analysis of IceTop data taken between June and October 2007 with the 26 station configuration of IceTop as shown in Fig. 1 is presented. The total livetime of the data is 3274.5h.

2 Air shower reconstruction

The observables of an air shower that can be measured by IceTop are the shower core position, angular direction, age, and shower size S_{125} . The latter is defined as the signal ex-



Correspondence to: F. Kislak
(fabian.kislak@desy.de)

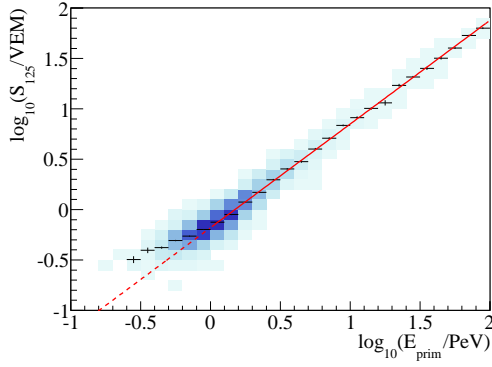


Fig. 2. Relation between primary energy and shower size for simulated proton showers with zenith angles up to 30° .

peptation value at a distance of $R = 125\text{m}$ from the shower core in units of Vertical Equivalent Muons (VEM) obtained from a fit of the lateral signal distribution described below. 1VEM is defined as the average signal generated inside an IceTop tank by a vertical 4GeV muon.

The signal expectation values are described by a lateral distribution function which has been derived from Monte Carlo simulations (Klepser et al., 2008):

$$S(R) = S_{125} \left(\frac{R}{125\text{m}} \right)^{-\beta - \kappa \log(R/125\text{m})}, \quad (1)$$

where R is the perpendicular distance to the shower axis. This function has five free parameters: the shower size S_{125} , slope β at $R = 125\text{m}$, curvature parameter κ , and the position of the shower core (x_c, y_c) . It turns out that $\kappa = 0.303$ is nearly independent of the primary particle mass and energy and has therefore been fixed in the fit. The reference radius $R_{\text{ref}} = 125\text{m}$ was chosen based on a study of the stability of the lateral fit. From air shower simulations it was found that β is linearly dependent on the shower age.

The shower direction is reconstructed by a fit of the signal times. The difference of the signal time at radius R and the arrival time of a plane through the shower core and perpendicular to the shower axis can be parametrized by a constant curvature function (Klepser et al., 2008):

$$\Delta t(R) = aR^2 + b \left(\exp\left(-\frac{R^2}{2\sigma^2}\right) - 1 \right) \quad (2)$$

with $a = 4.823 \times 10^{-4} \text{ns/m}^2$, $b = -19.41 \text{ns}$ and $\sigma = 83.5\text{m}$. This function has been obtained in a study of time residuals in experimental data. The only parameters of the fit are shower direction, core position and reference time T_0 at which the shower core reaches the ground. In the fit, all signal time fluctuations are assumed to be Gaussian.

Hence, the complete air shower reconstruction has the following parameters: the position of the shower core (x_c, y_c) , the shower direction θ and ϕ , the shower size S_{125} , and the

slope parameter β . Assuming a large correlation of the signals within the two tanks of one station and given that the fits of charges and times have four free parameters, five or more stations are required for a fit¹.

Following quality cuts have been applied to the reconstructed data in order to ensure that only well-reconstructed events enter the final sample:

- Only events with $2.0 \leq \beta < 4.5$ are used.
- The zenith angle has to be less than 46° .
- The reconstruction uncertainty on the core position is $\sigma_x = \sqrt{\sigma_x^2 + \sigma_y^2} < 20\text{m}$.
- The reconstructed core and the first guess core position (obtained by averaging the positions of triggered tanks weighted by the square root of their signal) has to be at least 50m inside the boundary of the array. Furthermore, it is required that the station containing the largest signal is not on the border of the array.

The containment cut is designed to be conservative. It reduces the overall efficiency ε (defined as the probability with which a shower whose core is inside the containment region will remain in the final event sample) but at the same time minimizes the number of showers outside the array that remain in the final sample. This is important since for a good energy determination a precise reconstruction of the core position is essential.

3 Energy estimation

The main observable sensitive to primary energy is the shower size S_{125} . Their relationship has been obtained from CORSIKA simulations using the SIBYLL and Fluka hadronic interaction models and is shown for protons with zenith angles up to 30° in Fig. 2. Above the threshold, where the efficiency is larger than 90% of its maximum value, primary energy and shower size are roughly proportional, while below $S_{125} \sim 1\text{VEM}$ the trigger condition biases the measurable shower sizes toward larger values. This happens because only showers fluctuating upwards will be able to trigger the array. The threshold of detectable energies increases for inclined showers and heavier primaries.

Above the threshold, the relationship between shower size and energy can be fitted by a simple line:

$$\log(S_{125}) = a + b(\log(E_{\text{prim}}/\text{PeV}) - 1). \quad (3)$$

Table 1 lists the dimensionless parameters a and b as a function of zenith angle for proton and iron primaries, as well as for the two-component model (Glasstetter et al., 1999) representing a simple case of a mixed composition.

¹A dedicated analysis is prepared for showers that trigger only three or four stations (Ruzybayev et al., 2009)

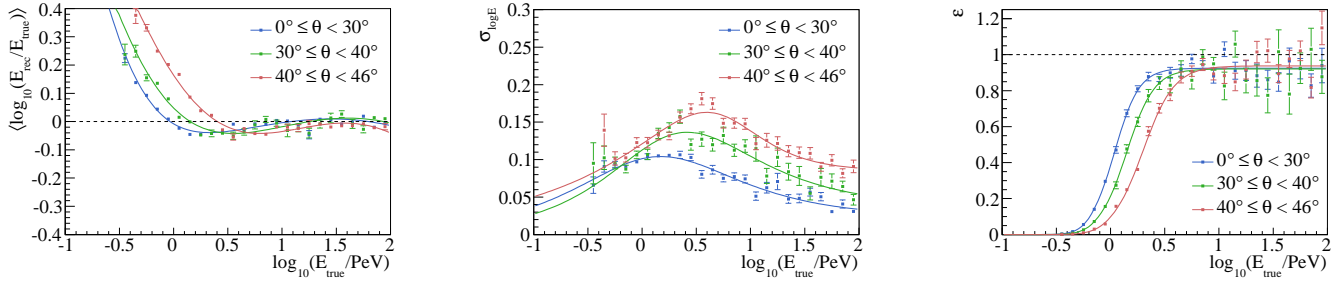


Fig. 3. The energy response of the IceTop detector obtained from air shower simulations assuming a two-component primary composition. The response is characterized by the energy bias (left), the resolution (center) and the overall efficiency (right).

Inverting Eq. (3) and using the parameters in Table 1, the primary energy of an air shower event can be calculated for different assumptions of the primary mass composition. Furthermore, it is important to note that inclined showers traverse more air than vertical ones. Due to the resulting attenuation the size of a shower of a given primary energy decreases with increasing zenith angle. One set of parameters is used per zenith angle bin, and no interpolation between them is done. The spectra for the different zenith angle ranges are reconstructed separately.

4 Detector response and unfolding

The measured energy spectra are affected by detection efficiency, energy bias in the threshold region, and bin-to-bin migration due to limited energy resolution. Detector effects can generally be expressed as

$$\mathbf{F}_{\text{reco}} = \mathbf{R}\mathbf{F}_{\text{true}} \quad (4)$$

where \mathbf{F}_{true} is the true energy spectrum, \mathbf{F}_{reco} the result of the measurement and \mathbf{R} is the response matrix describing the probability to measure a certain energy E_{reco} given the true primary energy E_{true} .

In this analysis, the detector response is characterised by three functions: energy bias $\langle \log(E_{\text{reco}}/E_{\text{true}}) \rangle(E_{\text{true}})$, resolution $\sigma_{\log E}(E_{\text{true}})$ and total efficiency $\varepsilon(E_{\text{true}})$. These functions are obtained from Monte Carlo simulations under the assumption that for a given $\log(E_{\text{true}})$, the logarithm of reconstructed energies, $\log(E_{\text{reco}})$, is normally distributed. The primary energy dependence of these quantities for the case of the two-component model is shown in Fig. 3. Fit functions are used to smooth out statistical fluctuations. At high energies the bias is very close to zero, while near the threshold the primary energy is overestimated as a result of the trigger bias described in the previous section. The resolution improves with increasing energy, eventually reaching a value of roughly 10%. The overall efficiency ε can become larger than 1.0 in cases where showers are selected despite their cores being located outside the containment region. The fact that it lies below 1 is due to the conservative containment cuts

Table 1. Dimensionless fit parameters of the relation between shower size and primary energy according to Eq. (3).

	a	b
Proton, $0^\circ \dots 30^\circ$	0.8499(21)	1.029(3)
Proton, $30^\circ \dots 40^\circ$	0.740(4)	1.075(6)
Proton, $40^\circ \dots 46^\circ$	0.560(4)	1.113(8)
Iron, $0^\circ \dots 30^\circ$	0.8122(24)	1.101(4)
Iron, $30^\circ \dots 40^\circ$	0.618(4)	1.140(8)
Iron, $40^\circ \dots 46^\circ$	0.411(4)	1.178(7)
Two-Component, $0^\circ \dots 30^\circ$	0.8379(18)	1.0517(29)
Two-Component, $30^\circ \dots 40^\circ$	0.685(4)	1.068(7)
Two-Component, $40^\circ \dots 46^\circ$	0.491(3)	1.096(6)

described in Sect. 2. The detector response for pure proton and iron primaries are similar, but reflect the fact that heavier primaries have a larger threshold energy.

Once the response matrices have been found, an unfolding algorithm (D'Agostini, 1995) is used to derive the final energy spectra. This algorithm employs an iterative procedure that avoids amplification of statistical fluctuations which can arise when simply inverting the response matrix \mathbf{R} .

5 The energy spectrum

Figure 4 shows the resulting energy spectra for three angular bands and three different composition models. Only showers with an efficiency of more than 90% of the maximum value were selected. As seen in Figures 4(a) and (b), assuming purely proton or iron primaries, the spectra in the three zenith angle ranges do not agree. Furthermore, the order becomes inverted when changing from light to heavy primaries. The reason for this is the varying angular dependence of shower attenuation for different primary masses. However, assuming an isotropic flux, the spectra obtained by analyzing showers from different zenith angle ranges should agree.

Assuming the Monte Carlo simulations correctly describe shower attenuation in the atmosphere, the three spectra will

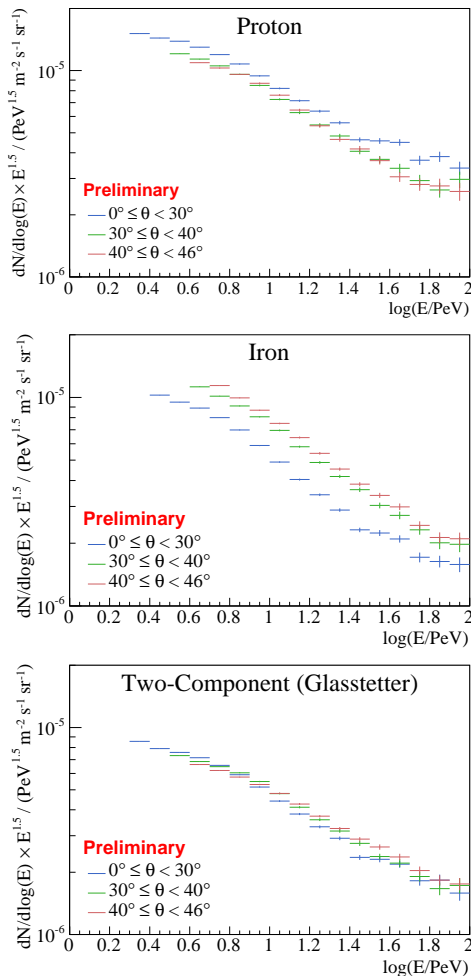


Fig. 4. Resulting cosmic ray energy spectrum obtained under different assumptions on the primary mass. The results obtained under a pure proton or iron assumption are not compatible with an isotropic flux since the spectra from different zenith angle ranges do not agree.

only align if the assumed composition corresponds to the one observed the data. Figure 4(c) shows the result for the two-component model. The three spectra clearly agree much better than in the other two cases. Therefore, our results are consistent with a mixed primary composition as determined by KASCADE (Antoni et al., 2005; Apel et al., 2009).

6 Conclusions

An update on the status of the cosmic ray energy spectrum analysis with IceTop has been presented. The preliminary energy spectrum is shown in Fig. 4 for different composition assumptions. These results have not yet been compared with other experiments since various systematic checks still remain to be performed. It has been demonstrated that the difference in attenuation of air showers initiated by particles

of varying primary mass can be used to distinguish alternative models for the chemical composition of cosmic rays, although this result still needs to be checked with different hadronic interaction models.

The basic assumption, isotropy of the cosmic ray flux, is the same as in the widely used method of Constant Intensity Cuts as described in Nagano et al. (1984). In contrast to that method, however, in the analysis presented here the attenuation of inclined showers is not derived from experimental data but from Monte Carlo simulations. In this way, information on the primary mass is preserved, at the cost of a larger dependence on air shower models.

The main strength of IceTop is the possibility to measure air showers at the surface in coincidence with high energy muons penetrating deep enough into the ice to trigger IceCube. The ratio between the two measurements is sensitive to the mass of the primary particle, as shown in Feusels et al. (2009). The method presented here is a systematically independent way to obtain information on the chemical composition of cosmic rays. It allows a verification of the detector performance and a cross-check of composition results obtained by the measurement of coincident events.

Edited by: T. Suomijarvi

Reviewed by: two anonymous referees

References

- Achterberg, A. et al. (IceCube Coll.): First year performance of the IceCube neutrino telescope, *Astropart. Phys.*, 26, 155–173, 2006.
- Antoni, T. et al. (KASCADE Coll.): KASCADE measurements of energy spectra for elemental groups of cosmic rays: Results and open problems, *Astropart. Phys.*, 24, 1–25, 2005.
- Apel, W. et al. (KASCADE Coll.): Energy spectra of elemental groups of cosmic rays: Update on the KASCADE unfolding analysis, *Astropart. Phys.*, 31, 86–91, 2009.
- D’Agostini, G.: A multidimensional unfolding method based on Bayes’ Theorem, *Nucl. Instrum. Meth. A*, 362, 487–498, 1995.
- Feusels, T. et al. (IceCube Coll.): Reconstruction of IceCube coincident events and study of composition-sensitive observables using both the surface and deep detector, in: *Proc. 31st Intern. Cosmic Ray Conf.*, Łódź, Poland, 2009.
- Gaisser, T.: *Cosmic Rays and Particle Physics*, Cambridge University Press, Cambridge, UK, 1990.
- Glasstetter, R. et al. (KASCADE Coll.): Analysis of electron and muon size spectra of EAS, in: *Proc. 26th Intern. Cosmic Ray Conf.*, 222, Salt Lake City, USA, 1999.
- Klepser, S. et al. (IceCube Coll.): First Results from the IceTop Air Shower Array, in: *Proc. 21st European Cosmic Ray Symp.*, Košice, Slovakia, 2008.
- Nagano, M., Hara, T., Hatano, Y. et al.: Energy spectrum of primary cosmic rays between $10^{14.5}$ and 10^{18} eV, *J. Phys. G Nucl. Partic.*, 10, 1295–1310, 1984.
- Ruzybayev, B. et al. (IceCube Coll.): Small air showers in IceCube, in: *Proc. 31st Intern. Cosmic Ray Conf.*, Łódź, Poland, 2009.